Available online at www.sciencedirect.com

SCIENCE DIRECT®

Earth and Planetary Science Letters 227 (2004) 17–35

EPSL

www.elsevier.com/locate/epsl

Magma genesis and mantle flow at a subducting slab edge: the South Sandwich arc-basin system

P.T. Leat[a,*], J.A. Pearce[b,1], P.F. Barker[a,2], I.L. Millar[a,c,3], T.L. Barry[b,c,4], R.D. Larter[a,5]

[a] *British Antarctic Survey, Madingley Road, Cambridge CB3 0ET, UK*
[b] *Department of Earth Sciences, Cardiff University, Cardiff CF10 3YE, UK*
[c] *Isotope Geosciences Laboratory, BGS, Keyworth NG12 5GG, UK*

Received 19 April 2004; received in revised form 21 July 2004; accepted 17 August 2004
Available online 21 September 2004
Editor: B. Wood

Abstract

The intra-oceanic South Sandwich subduction system is distinctive in having a narrow slab with slab edges at its northern and southern ends. We present new geochemical data to investigate magma genesis beneath the parts of the arc and back-arc segments that lie close to the two slab edges: Kemp and Nelson seamounts at the southern edge of the South Sandwich arc, and segments E1 and E2 in the south, plus segments E9 and E10 in the north, of the East Scotia Sea. In the arc, Kemp and Nelson seamounts exhibit enhanced subduction fluxes compared to the remainder of the arc. The southernmost (Nelson) has the isotope (low Nd and high Sr isotope ratios) and elemental (ultra-high Th and Ba and high Hf/Nd ratios) characteristics of a sediment melt, or supercritical aqueous fluid, component. The more northerly (Kemp) has the same characteristics as the remainder of the arc (high Nd and slightly raised Sr isotope ratios, high Nd/Hf ratios, high Ba/Th ratios), indicative of a fluid component derived mainly from subducted crust, but has a greater mass fraction of that component than the rest of the arc. In the back-arc basin, the slab-edge segments are generally fed by more fertile mantle (E-MORB in all but E1) than the segments in the centre of the basin (N-MORB). At the edges, segments furthest from the trench (E2, E9) have small subduction components while those nearer to the trench (E1, E10) have larger subduction components and slightly more depleted mantle. We argue that several processes were important at the slab edges: roll-back of the slab, forcing sideways flow of relatively enriched mantle into the mantle wedge; convergence of the arc with the back-arc spreading centre, imparting a greater subduction component into the back-arc lavas; and

* Corresponding author. Tel.: +44 1223 221432; fax: +44 1223 362616.
E-mail addresses: p.leat@bas.ac.uk (P.T. Leat), PearceJA@Cardiff.ac.uk (J.A. Pearce), pfbarker@tiscali.co.uk (P.F. Barker), i.millar@bas.ac.uk (I.L. Millar), tbarry@bgs.ac.uk (T.L. Barry), r.larter@bas.ac.uk (R.D. Larter).
[1] Tel.: +44 29 208 75124.
[2] Present address: 25 Church Street, Great Gransden, Sandy, Bedfordshire SG19 3AF, UK. Tel.: +44 1767 677081.
[3] Tel.: +44 115 936 3402.
[4] Tel.: +44 115 936 3134.
[5] Tel.: +44 1223 221573.

0012-821X/$ - see front matter
doi:10.1016/j.epsl.2004.08.016

anomalous heating of the subducting slab, increasing subduction fluxes and the contribution of sediment melts to the subduction component.

Keywords: subduction; geochemistry; back-arc basin; slab ends; mantle flow

1. Introduction

Traditionally, mantle flow, volatile migration and melt generation processes in subduction zones have been modelled as 2D phenomena that take place in a vertical plane that is perpendicular to subducting slabs, and forced by slab subduction [1–4]. However, earthquake shear wave splitting indicates that flow in mantle wedges can be trench-parallel [5,6]. Departure from mantle flow perpendicular to the slab is favoured where edges of slabs are being subducted. Such situations may be characterized by increase in roll-back of the trench toward the slab edge [7,8], and evidence from seismic anisotropy, magma production rates and geochemical tracing indicates that mantle flows from outside the arc-basin system into the mantle wedge [6,9,10]. Mantle flow around the edge of a subducting slab juxtaposes cold and hot elements of the subduction system, and allows ingress of mantle that is anomalous (for subduction systems) into the mantle wedge. Slab edge environments are therefore characterized by eruption of magmas with compositions that are anomalous with respect to normal volcanic arcs, including adakites (partial melts of basaltic slabs) [11], boninites (partial melts of normally refractory mantle) [12], and alkaline magmas (partial melts of enriched mantle) [13,14]. The South Sandwich subduction system is subducting slab edges at both its north and south ends, and is thus an important location for examining slab edge effects on subduction-related magmatism.

2. The South Sandwich arc-basin system

The South Sandwich system in the Southern Atlantic Ocean is one of the simplest of the world's arc-basin systems. As such, it provides a good 'natural laboratory' for studying the dynamic controls on subduction-related magmatism. The present system has been active at least since 15 Ma. It comprises a westward-subducting South American Plate, a primitive island arc (the South Sandwich arc), a back-arc basin (the East Scotia Ridge) and a fore-arc terrane (Fig. 1). The tectonics of the first three of these components are crucial to the objective of relating magmatism and geodynamics of the region.

The subducting plate is some 2000 km west of the Bouvet and Shona hot-spots. It was produced at the slow-spreading (13 mm/year full-rate) South America–Antarctic Ridge [15,16]. The subducted crust is older at the trench in the north (c. 83 Ma) than in the south (c. 27 Ma). Both north and south have similar thicknesses of siliceous ooze, but the north has additional calcareous sediment. Virtually all sediment arriving at the trench is subducted [17]. The convergence rate varies from 67 mm/year in the north to 79 mm/year in the south, and most of this motion is accommodated by rapid eastward roll-back of the trench [18]. The dip of the slab increases to about 75° below c. 60 km depth [19]. The geometry of the system is such that the South American Plate has to tear in the north in order to subduct, creating a major zone of seismic activity [20]. In the south, by contrast, the subduction ends at an active transform plate boundary and tearing need not, and does not, take place. A series of ridge–trench collisions has caused the southern end of the trench to migrate north with time [21].

The South Sandwich island arc can be seen from magnetic anomalies to lie mostly on 8–10 Ma back-arc ocean floor [22]. The volcanic arc itself is made up of seven main islands and several smaller islands and shoals. The main islands are the summits of volcanoes that rise 3 km above the surface of the ocean plate. The arc crust is 16–20 km thick [22], which is at the lower end for active arcs. The volcanic rocks vary in composition from basalts to rhyolites and from low-K tholeiitic through tholeiitic to calc-alkaline series. There are no obvious progressive changes in composition along the arc [23,24].

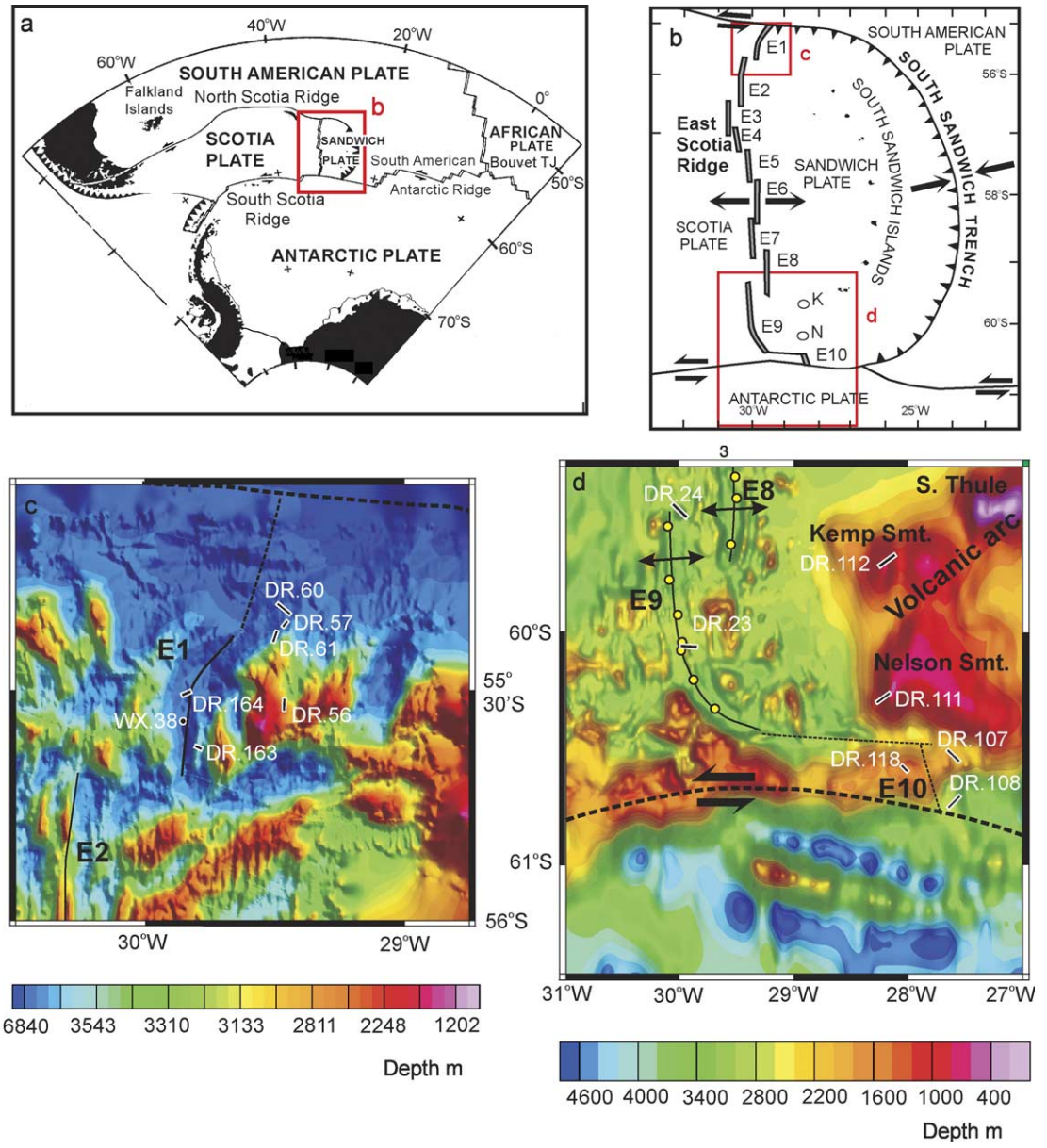

Fig. 1. Maps of the South Sandwich arc-basin system. (a) Regional tectonic map. (b) Sketch map of the Sandwich Plate showing positions of segments of the back-arc spreading centre (E1 to E10) and Kemp (K) and Nelson (N) seamounts. (c and d) Bathymetric maps, showing sample sites, of the northern and southern parts, respectively, of the East Scotia Ridge and volcanic arc. Both maps were derived by combining predicted bathymetry from satellite-derived altimetry [62] with HAWAII MR1 bathymetry for the area of the spreading centre [9]. In (d), samples reported by [26] in segments E9 and E8 are in yellow.

The East Scotia Sea back-arc basin formed over the past 15 Ma, and possibly more, by extension behind this east-migrating subduction zone [21,22]. Well-formed oceanic magnetic lineations demonstrate east–west extension at a rate of 62–70 mm/year [9,18]. The spreading centre consists of ten segments (from E1 in the north to E10 in the south) [9,25] (Fig. 1b). The ridge is rift-like in most segments, notably those in the

central part of the back-arc, which are also typically dominated by mid-ocean ridge (MORB)-like compositions [26]. In contrast, segments E2 and E9, near the north and south ends of the back-arc, respectively, are inflated, thought to be a response to inflow of mantle into the back-arc around both the north and south edges of the slab [9,27,28]. Shear-wave splitting of earthquakes centred beneath the northern part of the arc indicates that mantle deformation directions are locally parallel to the trench [29], indicating that mantle flow was also in this direction. In the south, the shallow bathymetry and absence of magnetic lineations suggest that true oceanic spreading in segment E9 commenced recently [28]. The crust on both sides of the segment is thought to consist of extended intra-oceanic arc similar to that forming the ~12–20-Ma Jane and Discovery Banks [28,30,31].

To date, the margins of the back-arc basin and island arc have not been investigated. This paper reports new geochemical data for samples from the northernmost segment (E1) and southernmost segment (E10) of the basin, and from two seamounts (Kemp and Nelson) from the southern extremity of the arc. The data are then used in conjunction with published data to examine the nature and effects of mantle flow around the north and south slab edges of the system.

3. Analytical methods

Major elements for most samples were analysed by XRF at the University of Keele, while samples DR.163.2-5 and DR.164.1 were analysed by a Cameca SX50 microprobe at the University of Kiel, and sample WX.38 was analysed by Cameca SX100 microprobe at the Open University. Trace elements were analysed by Perkin Elmer "Elan 6000" ICP-MS at the University of Durham and X-series Thermoelemental ICP-MS at Cardiff University using methods similar to those of [23] with calibration based on USGS international standards and dissolution by standard HF-HNO_3 digestion of 0.1 g of agate-crushed rock powder. Data are summarized in Table 1 and presented in full in the online Appendix.

Sr and Nd isotopic compositions were measured at the NERC Isotope Geosciences Laboratory, using the methods of [32]. Sr and Nd isotope compositions were measured on a MAT262 mass spectrometer. $^{143}Nd/^{144}Nd$ ratios are normalized to $^{146}Nd/^{144}Nd=0.7219$. During the period of analyses, the following standard results were obtained: La Jolla, 0.511860 ± 36 (2σ, 19 determinations); J&M, 0.511123 ± 32 (2σ, 57 determinations); NBS987, 0.710197 ± 42 (2σ, 256 determinations). The isotope data are given in Table 2.

4. Sample locations

Sample locations are shown in Fig. 1 and described in the online Appendix.

4.1. The back-arc basin at the northern subduction edge

Segment E1 is 65 km in length and forms the spreading arm of the RTF triple junction at the northern end of the East Scotia Ridge. Livermore et al. [9] carried out detailed bathymetry and side-scan sonar imaging of the northern end of the ridge (Fig. 1c). They found that Segment E1 has a chaotic backscatter pattern, and inferred that either the segment is a recent development or that extension is diffuse. They also deduced that the segment nucleated at the triple junction and then propagated southwards. The segment lies to the north of the tear in the subducting plate, which is at a latitude of about 55°50′ S. Thus it is underlain, not by the westward subducting plate, but by the downwarped plate north of the tear, which may account for its great depth and rifted nature.

Dredges DR.56-61 were recovered by RRS *Shackleton* in 1981 from the east flank of the axial rift of the segment (Fig. 1c). Three dredges, DR.57, 60 and 61 lay within 10 km of the most active locus of spreading, on north–west-facing rift slopes. Dredge DR.56 was from a seamount structure of unknown origin, 20 km from the centre of the rift. All the samples are from normally magnetized crust younger than 0.7 Ma [21,22]. After the exact location of the segment was identified, its central rift was sampled by RRS *James Clark Ross* in 1996 (sample WX.38) and 1997 (dredges DR. 163 and 164).

Although most samples have generally a fresh appearance and low LOI, all the samples from DR.57

Table 1
Selected elemental data for lavas from the north and south ends of the South Sandwich subduction system

Sample	SiO_2	TiO_2	MgO	Na_2O	Cr	Rb	Sr	Y	Zr	Nb	Ba	La	Ce	Pr	Nd	Sm	Eu	Gd	Tb	Dy	Ho	Er	Tm	Yb	Lu	Hf	Ta	Th	U
Segment E1																													
DR.56.4	51.40	0.72	8.80	2.14	312	4.41	151	16.0	50.9	3.86	53.0	3.02	7.38	1.12	5.55	1.67	0.64	2.02	0.38	2.44	0.52	1.50	0.230	1.49	0.23	1.29	0.230	0.40	0.115
DR.56.9	53.59	0.59	9.10	2.08	378	5.05	137	14.1	42.0	2.01	40.1	2.06	5.47	0.85	4.40	1.47	0.55	1.75	0.35	2.16	0.45	1.39	0.207	1.36	0.20	1.21	0.150	0.32	0.103
DR.57.20	62.01	1.22	3.53	5.35	1	0.23	83	28.8	61.8	1.18	5.7	2.49	7.62	1.34	7.47	2.63	0.67	3.45	0.67	4.49	0.97	2.80	0.420	2.69	0.41	1.98	0.080	0.31	0.445
DR.57.23	52.26	0.83	9.13	5.40	158	0.23	130	20.8	41.5	0.53	19.4	0.80	3.18	0.67	4.37	1.77	0.68	2.39	0.50	3.27	0.70	2.01	0.307	1.97	0.29	1.39	0.057	0.08	0.033
DR.57.25	56.05	1.01	6.93	6.51	19	0.17	22	22.5	68.5	1.20	5.1	1.79	6.09	1.04	5.84	2.09	0.66	2.71	0.55	3.62	0.77	2.27	0.350	2.27	0.35	1.93	0.087	0.22	0.107
DR.60.1	50.88	0.71	8.15	2.12	292	2.39	88	15.1	34.8	0.78	20.2	1.31	3.77	0.69	3.95	1.42	0.56	1.82	0.37	2.35	0.51	1.51	0.223	1.50	0.23	1.03	0.057	0.15	0.050
DR.60.3	53.04	0.61	5.70	2.21	63	5.38	124	15.8	38.4	0.53	42.5	1.28	4.11	0.71	4.03	1.47	0.57	1.87	0.37	2.44	0.54	1.55	0.243	1.58	0.24	1.20	0.053	0.25	0.087
DR.60.8	50.52	0.70	8.45	1.96	299	2.49	119	14.5	33.8	0.75	21.2	1.23	3.94	0.63	3.63	1.31	0.53	1.71	0.35	2.23	0.48	1.43	0.217	1.40	0.21	0.98	0.050	0.13	0.040
DR.61.1	54.46	0.73	5.65	2.57	57	5.25	148	17.7	45.7	1.69	31.4	2.68	7.01	1.08	5.41	1.84	0.70	2.40	0.43	2.80	0.60	1.75	0.266	1.76	0.28	1.33	0.097	0.31	0.119
DR.61.2	54.30	0.73	4.95	2.45	55	5.28	149	18.1	47.1	1.71	29.2	2.78	7.17	1.10	5.65	1.91	0.71	2.47	0.44	2.86	0.61	1.78	0.280	1.79	0.29	1.35	0.097	0.32	0.113
DR.61.8	55.18	0.79	7.04	4.70	80	2.26	110	20.3	41.5	0.71	31.4	1.94	5.97	1.04	5.59	2.15	0.78	2.91	0.52	3.38	0.71	2.04	0.302	1.96	0.30	1.39	0.059	0.17	0.064
DR.163.2	55.81	0.88	4.89	2.69	15	2.69	101	19.5	46.7	0.95	23.7	1.71	4.95	0.84	4.81	1.68	0.64	2.40	0.46	3.03	0.67	1.93	0.309	1.97	0.32	1.39	0.071	0.18	0.059
DR.163.3	53.21	0.59	6.96	2.07	178	2.18	92	15.3	34.5	0.65	17.9	1.24	3.64	0.63	3.57	1.28	0.51	1.83	0.34	2.40	0.52	1.53	0.240	1.56	0.25	1.03	0.045	0.13	0.047
DR.163.4	53.66	0.58	7.00	2.10	128	2.31	93	16.4	37.8	0.70	19.5	1.40	4.02	0.70	3.93	1.40	0.54	2.00	0.38	2.55	0.56	1.64	0.257	1.65	0.26	1.10	0.051	0.15	0.056
DR.163.5	54.22	0.59	6.73	2.12	192	1.79	92	14.8	33.9	0.64	20.0	1.42	4.05	0.66	3.68	1.28	0.50	1.91	0.35	2.37	0.52	1.50	0.239	1.52	0.25	1.03	0.047	0.19	0.074
DR.164.1	54.67	0.69	5.83	2.23	420	1.55	80	15.3	35.9	0.69	17.2	1.18	3.55	0.60	3.61	1.25	0.50	1.87	0.35	2.35	0.52	1.53	0.234	1.57	0.25	1.08	0.055	0.12	0.041
WX.38	56.13	0.74	6.14	2.49		3.20	196	33.2	83.2	2.68	44.0	4.70	12.56	1.96	10.68	3.19	1.20	4.02	0.76	5.50	1.22	3.30	0.549	3.39	0.50	2.44	0.060	0.50	0.120
Segment E9																													
DR.23.1	50.42	1.45	7.21	3.55	40	5.62	214	27.0	122.1	8.35	107.6	6.72	17.07	2.59	12.71	3.62	1.25	4.00	0.75	4.75	0.98	2.74	0.438	2.62	0.40	2.79	0.550	0.52	0.249
DR.23.2	50.35	1.46	7.36	3.39	34	6.25	214	29.8	124.5	8.58	94.7	6.97	17.54	2.67	13.25	3.80	1.31	4.17	0.80	5.01	1.03	2.91	0.467	2.76	0.42	2.87	0.560	0.56	0.245
DR.24.3	54.49	0.63	7.63	1.93	303	3.68	125	14.7	37.6	0.93	51.1	1.69	5.07	0.79	4.23	1.40	0.53	1.80	0.34	2.25	0.49	1.45	0.223	1.48	0.23	1.09	0.090	0.24	0.077
DR.24.11	53.98	0.62	8.32	1.84	320	3.46	128	14.8	38.5	0.97	49.0	1.89	5.40	0.84	4.31	1.42	0.54	1.76	0.35	2.31	0.49	1.46	0.230	1.51	0.24	1.01	0.060	0.27	0.080
DR.24.24	53.13	0.92	5.08	2.83	99	5.45	167	21.8	65.1	1.45	66.5	3.00	8.70	1.39	7.24	2.31	0.84	2.89	0.53	3.45	0.75	2.19	0.355	2.11	0.33	1.79	0.095	0.38	0.120
Segment E10																													
DR.107.11	54.30	1.43	3.40	4.53	15	5.11	249	33.3	128.1	4.87	90.9	6.21	16.26	2.55	12.32	3.94	1.40	4.83	0.84	5.21	1.12	3.19	0.480	3.11	0.49	3.06	0.315	0.63	0.260
DR.107.12	52.26	1.42	5.56	3.52	304	5.54	186	25.7	99.2	3.32	46.1	4.15	11.86	1.95	9.70	3.10	1.07	3.47	0.67	4.29	0.90	2.53	0.405	2.43	0.38	2.32	0.227	0.32	0.160
DR.107.13	53.30	1.97	2.80	4.45	19	12.17	202	39.5	153.3	5.87	65.5	6.48	18.23	3.01	14.83	4.82	1.72	5.91	1.00	6.33	1.33	3.75	0.560	3.60	0.56	3.53	0.368	0.47	0.180
DR.107.14	50.87	1.85	2.74	6.61	7	9.79	196	41.2	163.6	6.20	116.6	7.12	19.90	3.28	16.21	5.06	1.72	5.51	1.06	6.67	1.39	4.03	0.644	3.87	0.60	3.72	0.404	0.54	0.204
DR.107.40	53.78	2.03	2.63	4.76	1	10.49	195	40.7	160.5	5.95	68.2	6.88	19.52	3.26	15.91	4.95	1.69	5.44	1.05	6.53	1.38	3.89	0.626	3.75	0.59	3.67	0.387	0.51	0.190
DR.108.11	54.79	1.11	3.87	3.23	27	7.43	205	25.9	98.6	4.49	71.6	5.03	13.05	2.02	9.65	3.05	1.11	3.72	0.65	4.16	0.87	2.57	0.390	2.53	0.40	2.39	0.289	0.54	0.190
DR.108.13	55.14	1.12	3.77	3.41	29	7.86	200	24.8	95.5	4.36	108.1	5.01	12.81	2.01	9.57	2.89	1.02	3.25	0.62	4.03	0.84	2.43	0.398	2.44	0.38	2.24	0.278	0.54	0.186
DR.108.P2	55.18	1.11	3.86	3.37	29	7.20	199	25.1	96.3	4.36	63.9	5.20	13.40	2.08	9.91	3.01	1.03	3.31	0.64	4.09	0.87	2.51	0.410	2.49	0.39	2.32	0.286	0.54	0.192
DR.108.P6	55.05	1.12	3.16	3.55	26	7.15	195	25.8	100.3	4.56	133.7	5.16	13.28	2.06	9.81	3.03	1.06	3.33	0.65	4.16	0.88	2.56	0.415	2.56	0.40	2.38	0.292	0.57	0.198
DR.118.1	53.05	1.67	2.84	3.55	4	6.66	223	27.7	97.5	5.23	84.6	5.68	15.32	2.40	11.81	3.62	1.29	4.01	0.77	4.89	1.00	2.85	0.455	2.73	0.42	2.38	0.350	0.61	0.211
DR.118.3	53.43	1.65	2.75	3.81	4	6.47	222	30.2	99.6	5.33	70.4	6.08	16.13	2.55	12.44	3.77	1.35	4.21	0.80	5.07	1.05	2.95	0.479	2.86	0.44	2.42	0.350	0.64	0.196
DR.118.4	52.69	1.65	2.68	3.59	1	6.99	231	30.6	100.5	5.53	79.8	6.04	15.98	2.51	12.07	3.91	1.43	4.77	0.81	5.06	1.06	3.00	0.450	2.89	0.44	2.46	0.348	0.63	0.200
Nelson Seamount																													
DR.111.2	65.15	0.65	1.29	3.37	30	40.31	158	31.0	112.1	4.36	312.4	11.30	25.20	3.34	14.59	3.68	0.94	4.01	0.75	4.82	1.03	3.04	0.507	3.13	0.50	3.14	0.321	4.36	1.205
DR.111.14	64.97	0.65	1.41	3.40	19	34.60	157	25.8	98.1	3.88	225.5	9.84	22.50	2.92	12.80	3.20	0.83	3.52	0.64	4.12	0.89	2.59	0.433	2.68	0.43	2.75	0.282	3.62	1.042
DR.111.182	65.49	0.62	1.29	3.38	14	39.73	156	30.6	109.1	4.38	293.9	11.45	25.23	3.28	13.71	3.71	0.95	4.27	0.76	4.79	1.02	3.05	0.470	3.13	0.49	3.16	0.309	4.33	1.200
Kemp seamount																													
DR.112.1A1	53.06	0.69	4.48	2.02	50	5.07	167	13.9	29.1	0.57	100.2	2.19	6.15	0.95	5.01	1.56	0.56	1.79	0.35	2.33	0.50	1.44	0.237	1.48	0.23	0.87	0.035	0.44	0.144
DR.112.6a	50.83	0.51	5.64	1.06	179	6.52	197	12.6	24.5	0.43	63.0	2.07	5.51	0.81	4.12	1.39	0.52	1.73	0.31	1.99	0.43	1.25	0.190	1.27	0.21	0.78	0.036	0.47	0.150
DR.112.31	49.96	0.64	5.22	1.59	63	5.09	156	14.3	26.4	0.52	90.5	2.00	5.51	0.89	4.65	1.53	0.56	1.75	0.36	2.33	0.51	1.48	0.244	1.52	0.24	0.85	0.032	0.40	0.144

Table 2
Sr, Nd and Pb isotopic data

Sample	$^{87}Sr/^{86}Sr$	$^{143}Nd/^{144}Nd$	$^{206}Pb/^{204}Pb$	$^{207}Pb/^{204}Pb$	$^{208}Pb/^{204}Pb$
Segment E1					
DR.56.4	0.703239	0.513007	18.3703	15.5534	38.1771
DR.56.9	0.703398	0.512999	18.5535	15.5702	38.4502
DR.57.20	0.704082	0.513083	18.4810	15.5573	38.2130
DR.57.23	0.704122	0.513133	18.4784	15.5656	38.2228
DR.57.25	0.703344	0.513075	18.4366	15.5551	38.1716
DR.60.1	0.704538	0.513049	18.5637	15.6033	38.4208
DR.60.3	0.703583	0.513012	18.5648	15.6098	38.4777
DR.60.8	0.703333	0.513054			
DR.61.1	0.703325	0.513067	18.3472	15.5796	38.2090
DR.61.8	0.703706	0.513087	18.5038	15.5796	38.3577
DR.163.2	0.703283	0.513043	18.3147	15.5532	38.1356
DR.163.3	0.703357	0.513041	18.2985	15.5697	38.1592
DR.163.4	0.703338	0.513044	18.3460	15.5723	38.2317
DR.163.5	0.703522	0.513004	18.2358	15.5570	38.0792
DR.164.1	0.703310	0.513034	18.4242	15.5655	38.2595
Segment E9					
DR.23.2	0.703001	0.513045	18.0223	15.4963	37.6753
Segment E10					
DR.107.12	0.703063	0.513108	17.9055	15.4821	37.5798
DR.107.14		0.513128	17.9391	15.5194	37.6914
DR.108.P2		0.513060	18.1625	15.5608	38.0147
DR.108.13	0.703175	0.513061	18.1958	15.5413	37.9976
DR.118.1		0.513044			
Nelson seamount					
DR.111.2	0.704841	0.512673	18.7245	15.6211	38.6285
DR.111.14	0.704857	0.512690	18.7185	15.6370	38.6577
Kemp seamount					
DR.112.6A	0.703704	0.512980	18.4180	15.5800	38.2929
DR.112.31			18.4759	15.5696	38.3059

and sample DR.61.8 have experienced greenschist facies alteration. $^{87}Sr/^{86}Sr$ ratios of these samples and DR.60.1 are have been increased by interaction with seawater (Table 2), and are not discussed. Two of the altered samples from Dredge DR.57 are more fractionated than others from segment E1; one is an andesite and the other a dacite.

Segment E2 has already been described in detail [27]. Samples are predominantly basalts and basaltic andesites and subdivide into two groups. The most common has major element characteristics similar to those of MORB, with high Na8. A subset, however, has low Na8 and a significantly greater subduction component.

4.2. The back-arc basin at the southern subduction edge

Segment E9 (Fig. 1d) is the southernmost major segment of the East Scotia Ridge. It is 105 km long and well defined magnetically, bathymetrically, and by side-scan sonar imaging [9,22,28]. It is an anomalous, curved segment, that is rift-like and up to 3.6 km deep along much of its length. A ~40-km-long axial ridge rises ~500 m above the valley floor in the centre of the segment. Ocean spreading started along the segment more recently than the rest of the East Scotia Ridge [22,28]. Fretzdorff et al. [26] published analyses of glasses from the segment. We present additional, new data for dredge DR.23 recovered by RRS *Shackleton* in 1974 from the axial ridge of the segment. We also re-analysed DR.24, from an anomalous seamount-like structure at the northern termination of the segment. It is compositionally more similar to Segment 8 and may be derived from pre-existing attenuated arc lithosphere. We do not, therefore, consider it further in this paper. These new analyses update the early work on these samples [33–38].

Segment E10 is poorly surveyed. It is connected to Segment E9 and to the trench by transform faults [21,39] (Fig. 1d). Its position and orientation are constrained by unpublished British Antarctic Survey GLORIA data. Dredges 107 and 108 were recovered on the RRS *Discovery* 1984-5 cruise, and Dredge 118 was recovered by the RRS *John Biscoe* in 1987. Comparison of dredge site locations with the subsequently determined location of segment E10 indicates that sites DR.107 and DR.108 originated at the E10 spreading axis. Sites DR.107 and DR.108 lie on the present east flank of E10. Site DR.118 lies some 20 km from E10 and is probably related to the spreading centre. Rocks from E10 are typically basalts, with some basaltic andesites. They are all vesicular.

4.3. The South Sandwich arc at the Southern subduction edge

Kemp and Nelson seamounts represent the southernmost expression of the South Sandwich arc (Fig. 1b,d) and were dredged by RRS *Discovery* in 1985 [21,39].

Kemp Seamount is situated 50 km west–south–west of Thule Island, the southernmost of the South Sandwich Islands. It lies on a bathymetric continuation of the volcanic arc, and is a similar distance from the trench as other volcanoes of the arc. It is situated 70 km north of the southern edge of the subducting plate, as delimited by earthquake foci. It rises to within ~80 m of sea level and is therefore considered volcanically active (old seamounts are planed by icebergs to >500 m below sea level) [39]. Dredge DR.112 sampled the north slope of the seamount and recovered tholeiitic basalts and basaltic andesites, all significantly fractionated (from 5.6 to 4.5 wt.% MgO). With 0.23–0.29 K_2O, all classify as low-K tholeiites or tholeiites.

Nelson Seamount, situated 90 km southwest of Thule Island, is the southernmost known volcanic edifice of the arc and overlies the southernmost earthquake foci associated with the trench [39], and so is interpreted to overlie the edge of the subducting slab. It is situated trenchward of the trend of most of the volcanoes of the arc. It rises within 500 m of sea level, does not have a flat top planed by icebergs [39], overlaps young faults [21] and is thought to have been recently active. Dredge DR.111 sampled the east flank of the seamount. The three Nelson Seamount samples are dacites, and are compositionally similar to the calc-alkaline (medium-K) group of volcanic rocks from the South Sandwich arc [23].

5. Geochemical comparison between 'normal' and subduction-edge lavas

Here, we compare 'normal' compositions, defined as those from the centre of the arc-basin system with those from the edges. Comparison is made through four projections: multi-element geochemical patterns (Fig. 2); Th and Ba enrichments relative to Nb (Fig. 3); and Nd–Sr isotope ratios (Fig. 4).

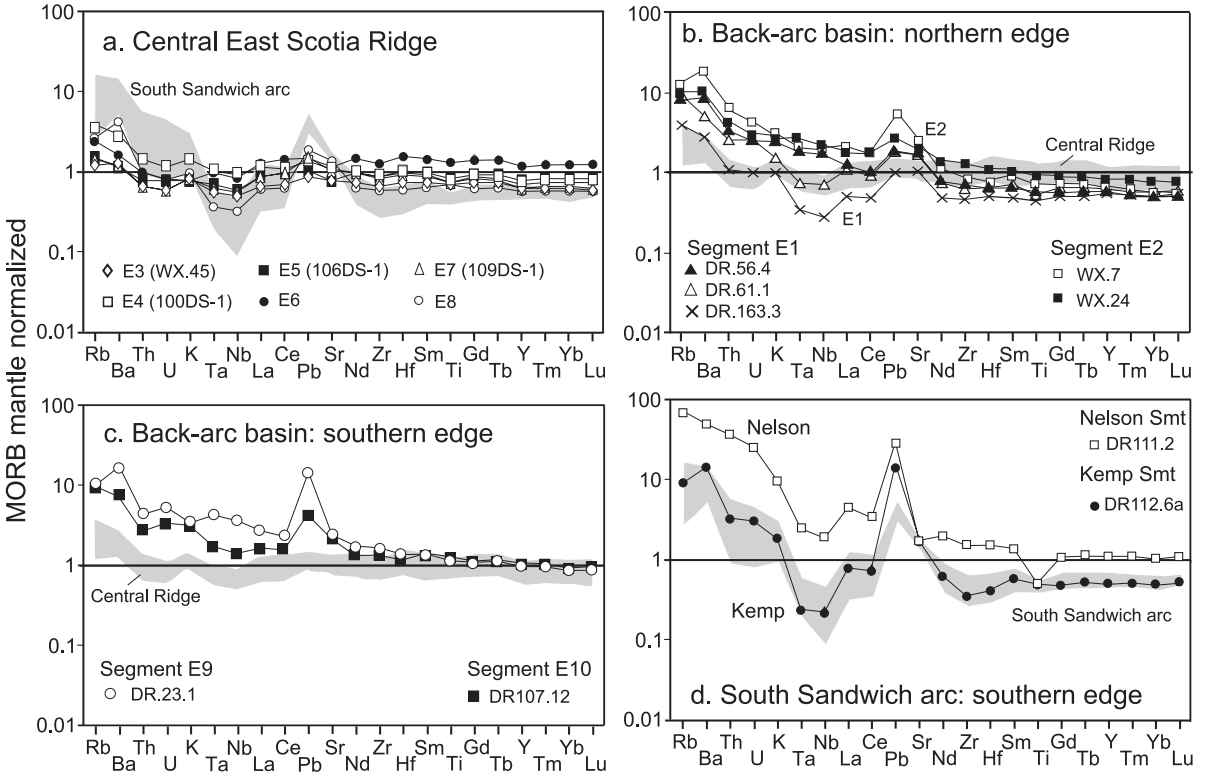

Fig. 2. MORB normalized [42] multi-element plots for samples from the north and south edges of the South Sandwich subduction system compared to the central parts of the arc and back-arc basin. Data from this paper and [24,26,27].

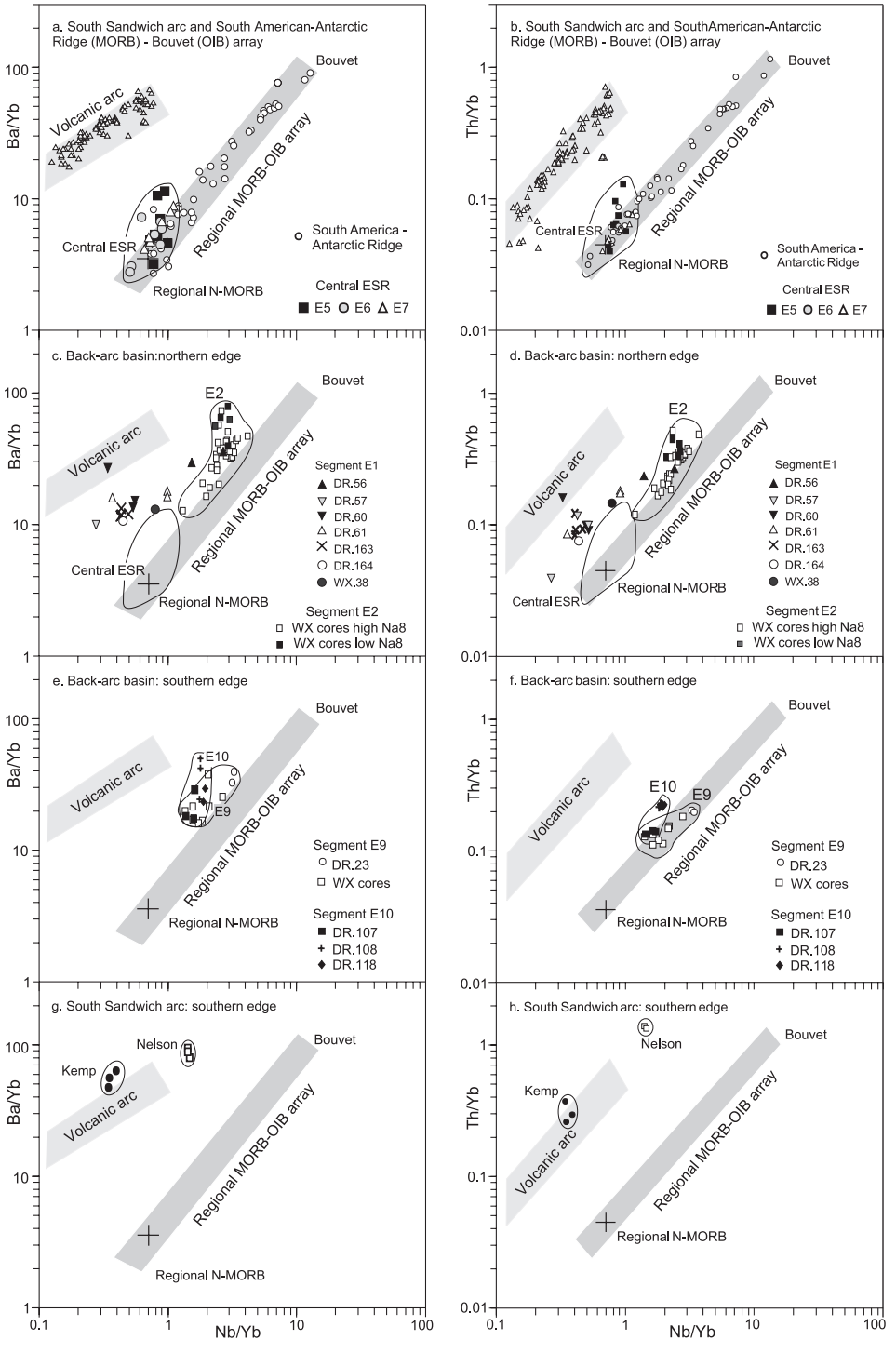
a. South Sandwich arc and South American-Antarctic Ridge (MORB) - Bouvet (OIB) array
b. South Sandwich arc and SouthAmerican-Antarctic Ridge (MORB) - Bouvet (OIB) array
c. Back-arc basin:northern edge
d. Back-arc basin: northern edge
e. Back-arc basin: southern edge
f. Back-arc basin: southern edge
g. South Sandwich arc: southern edge
h. South Sandwich arc: southern edge
Ba/Yb
Th/Yb
Nb/Yb
Bouvet
Volcanic arc
Regional MORB-OIB array
Regional N-MORB
Central ESR
South America - Antarctic Ridge
E2
E9
E10
Nelson
Kemp
Segment E1
DR.56
DR.57
DR.60
DR.61
DR.163
DR.164
WX.38
Segment E2
WX cores high Na8
WX cores low Na8
Segment E9
DR.23
WX cores
Segment E10
DR.107
DR.108
DR.118

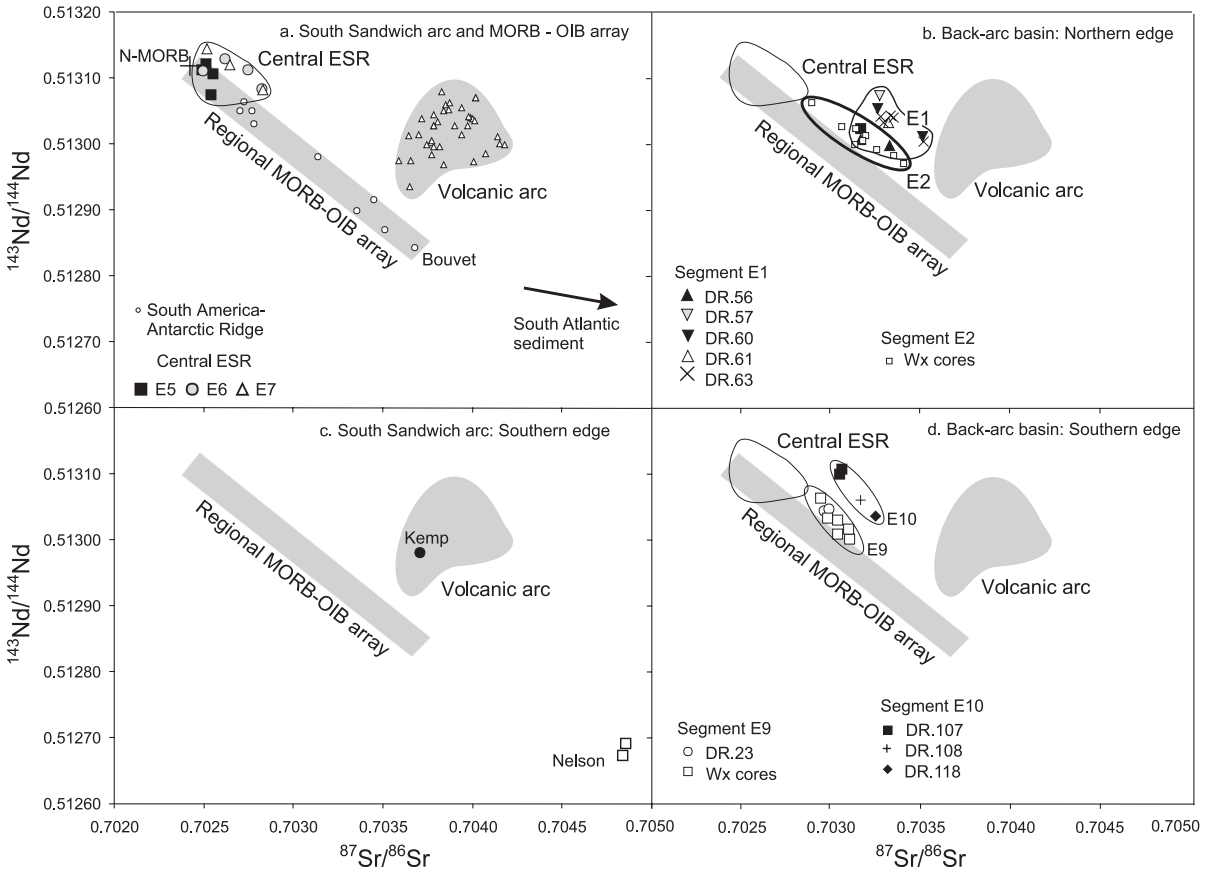

Fig. 4. Plots of $^{87}Sr/^{86}Sr$ versus $^{143}Nd/^{144}Nd$ for samples from the South Sandwich arc and back-arc, and regional MORB. Data sources for the South Sandwich arc and East Scotia Ridge in Fig. 3 and [40]. The regional MORB-OIB array is defined by samples from the South America–Antarctic Ridge [49]. Altered samples from segment E1 showing evidence for post-eruption increase in $^{87}Sr/^{86}Sr$ (DR.57.20, DR.57.23, DR.60.1, DR.61.8) are not plotted.

5.1. Compositions at the centre of the arc-basin system

MORB-normalized multi-element plots (Fig. 2a) highlight the overall trace element characteristics of the arc and central back-arc basin.

The islands of the South Sandwich arc have typical subduction patterns with selective enrichments in all the subduction-mobile elements (Rb, Ba, Sr, Pb, U, Th, LREE), giving the characteristic Nb,Ta anomalies. The extent of the enrichment increases from the low-K tholeiitic lavas (which form the lowermost part of the shaded area in Fig. 3a), through the tholeiitic to the calc-alkaline lavas (which form the uppermost part of the shaded area).

In the central basin, segments E5, E6 and E7 display patterns close to the sub-horizontal patterns followed by N-MORB, though sometimes with small enrichments in the most subduction-mobile elements such as Rb, Ba and Pb. Segments E4 and, particularly,

Fig. 3. Plots of Ba/Yb versus Nb/Yb and Th/Yb versus Nb/Yb for samples from the South Sandwich arc and back-arc, and regional MORB. In (a and b), regional MORB is defined by the South America–Antarctic Ridge forming an array between regional N-MORB and Bouvet Island (authors' unpublished data). This array is unaffected by Neogene subduction. The central segments of the East Scotia Ridge, E5, E6 and E7 plot within this array. In the remaining panels, data from segments near the ends of the East Scotia Ridge and Kemp and Nelson seamounts are shown. Altered samples showing evidence for Ba loss are not plotted. Data sources are [23,24,26,27,50]. Regional N-MORB is defined as having Nb/Yb=0.7, and the same Ba/Yb and Th/Yb ratios as the South America–Atlantic Ridge samples with this Nb/Yb ratio.

E8 are dominated by samples with subduction zone signatures [26], which are broadly similar to those of the arc though of smaller magnitude. Segment E3 has characteristics of both E4 and E5.

Closer examination of the Ba, Th, Nb part of the patterns is performed in Fig 3a and b. Yb is used as a normalizing factor for all three elements to reduce the effects of fractional crystallization and crystal accumulation [3]. Ba, Th and Nb have similar distribution coefficients for melting and fractional crystallization so that MORB forms a diagonal array on these projections with a slope close to unity. Thus, the subduction-unmodified lavas from the South America–Antarctic Ridge, considered on the basis of isotopic fingerprinting to belong to the same mantle domain as the arc and basin lavas [40], define the local MORB arrays of increasing Ba/Yb and Th/Yb with increasing Nb/Yb. The influence of the Bouvet plume means that the lavas are all enriched relative to N-MORB, although there is evidence that the enriched component decreases in magnitude with distance from the plume. The local MORB array has slightly higher Ba/Nb and Th/Nb ratios than the global average MORB; this may be explained by contamination of the mantle by Mesozoic subduction beneath Gondwana before opening of the South Atlantic [41].

For the central part of the basin, many lavas from MORB-like segments E5, E6 and E7 [26] plot within, or on a linear extension of, the mantle array in Fig. 3a and b. Some of the data lie at the depleted end of that trend, close to the Nb/Yb ratio of mean N-MORB [42] and can be interpreted as being derived from depleted mantle of the same mantle domain with no subduction zone addition. Other data extend to slightly higher contents of Ba and Th, indicating a small subduction input.

The main South Sandwich arc lavas are displaced from the MORB array to much higher concentrations of the subduction-mobile elements, Ba and Th. The inference is that Nb/Yb ratios are unaffected, or little affected, by additions of components during subduction, whereas increases in Ba/Yb and Th/Yb reflect addition of slab-derived components [23]. These components are widely thought to be aqueous fluids, often considered to be largely crustally derived, and a siliceous fluid (supercritical fluid or melt), often thought to be largely sediment-derived [3,23,24,43,44]. Ba is abundant in both components but Th is thought to predominate in the siliceous component. Addition of a variable subduction component to a constant mantle source gives a vertical trend on the diagrams as only Th and Ba are added while Nb and Yb remain nearly constant. Addition of a constant subduction component to a variable mantle source gives a negative, flat or shallow positive slope as depleted mantle (with lowest Nb) is affected more than enriched mantle. Addition of a subduction component followed by variable melting, such as dynamic melting, gives a trend parallel to but displaced from the MORB array [23].

The volcanic arc has up to about 10 times higher Th/Nb and up to 15 times higher Ba/Nb than the regional MORB arrays because of addition of Th and Ba from the subducting slab and sediments. The trends formed by the arc samples run sub-parallel to the regional MORB array for Th (Fig. 3a). However, for Ba (Fig. 3b), the trend diverges from the regional MORB array towards low Nb/Yb ratios, indicating that a combination of mantle depletion and subduction zone enrichment may have operated.

Isotope covariations permit similar petrogenetic interpretations (Fig. 4a). For example, for the $^{87}Sr/^{86}Sr$–$^{143}Nd/^{144}Nd$ isotope diagram, the South America–Antarctic Ridge gives a well-defined mantle array, which extends from a Bouvet Island composition towards that of N-MORB. The main South Sandwich arc forms a field to the right of this array as a result of addition of fluids with high Sr/Nd ratios from the subduction zone [23]. Samples from East Scotia Ridge segments E5, E6 and E7 that plot in the trace element mantle array in Fig 3a and b, also plot within the $^{87}Sr/^{86}Sr$–$^{143}Nd/^{144}Nd$ mantle array in Fig. 3a. Similarly, those plotting to higher Ba and Th show a selective displacement to higher $^{87}Sr/^{86}Sr$ for a much smaller change in $^{143}Nd/^{144}Nd$ and lie between the arc field and the MORB array.

5.2. Compositions at the northern edge of the back-arc basin

The patterns in Fig. 2b demonstrate that the two segments at the northern edge, E2 [27] and E1 (this paper) are geochemically distinct, both from each other and from most samples from the central basin. Most high-Na samples from E2 (i.e., the most MORB-

like) have higher concentrations of incompatible elements than samples from E3 to E7, indicative of a more enriched mantle source compared with the central basin [27]. They also have a small selective enrichment in the subduction-mobile elements, most apparent in the positive Pb spike. Low-Na samples from E2 (e.g. WX.7) have a greater subduction signature.

However, E1 samples have characteristics more like those of the arc than the back-arc. All E1 samples (except the MORB-like WX.38) are depleted in Yb, Ti and the heavy REE relative to N-MORB, and most have negative anomalies of Nb and Ta linked to enrichment of the subduction-mobile elements. Sample DR.56.4 is the least arc-like sampled from the segment, approaching the E-MORB-like patterns of Segment E2.

On the element ratio plots in Fig. 3c–d, samples from E2 have high Nb/Yb ratios and plot along the regional MORB array indicating that they also have an enriched mantle source relative to N-MORB. Most plot slightly above the mantle array indicating a small subduction component, although the low-Na set has greater subduction signatures [27]. Segment E1 has a wide range of compositions, including one identical to the arc (DR.60.3), and one (DR.56.4) with an enriched mantle source. Most samples have Nb/Yb ratios that are more depleted than E2 samples but more enriched than N-MORB, and are displaced from the MORB array to higher concentrations of the subduction-mobile elements Ba and Th.

Isotopically, the samples from Segment E2 again plot along the mantle array with small displacements to higher $^{87}Sr/^{86}Sr$ (Fig. 4b). By contrast, lavas from Segment E1 have larger displacement to higher $^{87}Sr/^{86}Sr$. The isotopic systematics therefore support the inferences made on the basis of Fig. 3c–d, namely that segment E1 is more depleted than Segment E2 overall, but with a greater subduction component.

5.3. Compositions at the southern edge of the back-arc basin

The patterns in Fig. 2c show that most of Segment E9 has high Nb–Ta, E-MORB-like compositions which dominate the axial high of the segment [26]. Like E2, it also carries a subduction component, as indicated most obviously on the pattern by its positive Pb spike. Samples from segment E10 vary little, and are similar to E-MORB but have significant peaks at Rb, Ba, K and Pb.

On the element ratio plots in Fig. 3e–f, lavas from Segment E9 plot as a tight cluster in a similar field to the high-Na lavas from E2. They are therefore similarly related to enriched (E-MORB) mantle sources with a small subduction addition. Segment E10 samples also require an enriched source, though less enriched than that of E9, and are displaced further from the MORB array indicating that they require a greater subduction component.

Isotope systematics again support the inferences made from the trace elements (Fig. 4b). E9 plots within the regional array, with a small displacement to higher $^{87}Sr/^{86}Sr$, whereas E10 plots closer to N-MORB, but with a larger displacement.

5.4. Compositions at the southern edge of the South Sandwich arc

Trace element patterns (Fig. 2d) show that Kemp and Nelson seamount samples clearly belong geochemically to the volcanic arc. Kemp lies at the uppermost end of the arc field. Nelson is more enriched in all elements, in part because it is more silica rich. Correcting for fractional crystallization, however, still has the Nelson seamount with a pattern which lies above the main South Sandwich arc.

Fig. 3g–h demonstrates that both seamounts are even more distinct than is apparent on the multi-element patterns. Both have high Ba/Yb and high Th/Yb ratios and both are clearly very strongly affected by subduction components. The Kemp samples plot within the volcanic arc array with respect to Th (Fig. 3h), but above the volcanic arc array with respect to Ba (Fig. 3g). This is consistent with a higher fluid flux than the rest of the arc. The Nelson dacites plot along a continuation of the volcanic arc trend to high Nb/Yb, moderately high Ba/Yb and very high Th/Yb ratios. Their Th/Nb ratios are the highest known in the South Sandwich subduction system.

In the isotope plot (Fig. 4c), the Kemp Seamount basalt plots within the field of the volcanic arc—which is consistent with its arc-like trace element ratios. However, the Nelson Seamount dacite has higher $^{87}Sr/^{86}Sr$ and significantly lower $^{143}Nd/^{144}Nd$ (0.512690) than any known South Sandwich arc

sample. It plots just to the right of the regional MORB array, has significantly lower $^{143}Nd/^{144}Nd$ than the Bouvet OIB component. Significantly, it plots towards the composition of local sediment, indicating a much larger sediment signal than elsewhere. This observation is supported by the Pb isotope data (given in the data table but not plotted here): of all the arc lavas, only Nelson plots within the field of subducted sediment. We examine this anomalous composition in more detail in the next section.

6. Further evidence for sediment melting at the southern edge of the South Sandwich arc

To examine the nature of the subduction component further, we have modelled the $^{143}Nd/^{144}Nd$–$^{87}Sr/^{86}Sr$ variations (Fig. 5). The shaded array represents the range of MORB compositions from the Bouvet mantle domain. M1, average back-arc basin N-MORB basalt from segments 5 to 7, represents the depleted end member of the mantle wedge. M3, average back-arc basin E-MORB from Segment 9 represents the enriched end-member of the mantle wedge. M2, depleted MORB from the South American–Antarctic Ridge represents the fresh subducting oceanic crust. We assume that seawater interaction has increased the Sr isotope ratio of M2 by 0.001 to give the subducting crust composition, C. The sediment composition modelled is siliceous ooze, S. The 'sediment–crust mixture' line, C–S from [23], then represents the composition of the subducted material and is nearly a straight line because altered crust and sediment have similar Sr/Nd ratios. To model the composition of 'normal' South Sandwich arc magmas, it is thus necessary to invoke convex-up mixing lines between a point on the mantle array and a point on the sediment–crust mixing line, i.e. Sr/Nd ratios must be high. Given the high percentage of subducted Sr in the South Sandwich lavas (calculated as c. 80% on average [23]), the Sr isotope ratio of the bulk subduction component must be not much more than the ratio in the arc lavas, typically 0.7035–0.7045. Thus, mixing lines between mantle wedge and

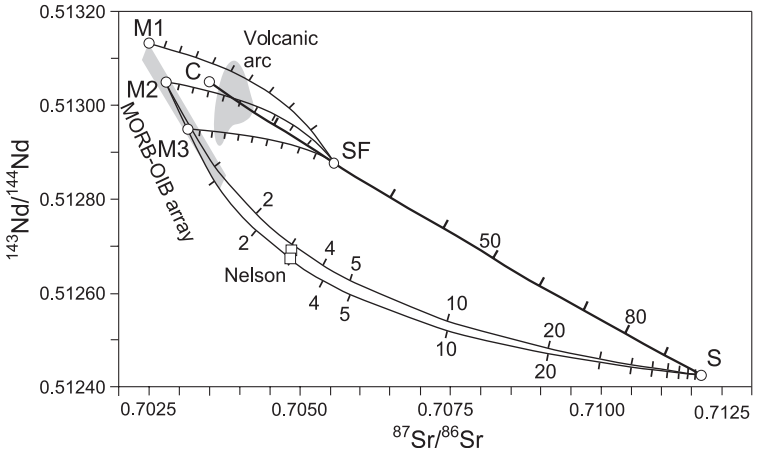

Fig. 5. Model for $^{87}Sr/^{86}Sr$ versus $^{143}Nd/^{144}Nd$ variations in the South Sandwich subduction system. The shaded fields for the regional MORB-OIB array and the South Sandwich arc are from Fig. 4. Subduction components are fall along the mixing curve between subducted igneous crust (C) and sediment (S: siliceous ooze, sample DR.113.3, author's unpublished data). The position of C is typical N-MORB of the South American–Antarctic Ridge, with allowance made for increase in for $^{87}Sr/^{86}Sr$ resulting from sea-floor alteration [23]. The Sr-bearing subduction flux (SF) is constrained to be near the crustal end-member. Three mantle end members are depleted MORB mantle (M1), typical MORB mantle (M2) and enriched MORB mantle (M3). The three convex-up curves model mixing of these mantle end-members with a subduction flux having high Sr(SF)/Sr(mantle) ratios of 0.8 to Nd(SF)/Nd(mantle) ratios of 0.3. These values are in accord with proportions of overall enrichments in the arc [23]. The high Sr/Nd of SF suggests that it is transported as a low-temperature fluid. The two concave curves show mixing of subducted sediment or a sediment-derived melt with typical MORB mantle, in order model the Nelson dacites. For both curves, Sr(S)/Sr(mantle) ratios are 10. Nd(S)/Nd(mantle) ratios are 40 for the upper curve and 50 for the lower curve. Sr is therefore much less abundant in component S used to derive the curves than its actual value in the subducting sediment. This implies that Sr was lost during release of an aqueous fluid (or that Sr was weakly compatible during melting).

subduction component must intersect the crust–mantle mixing line much closer to the altered crust end-member than to the sediment. Fig. 5 shows typical mixing lines for the end-member mantle wedge compositions. Kemp seamount plots within these lines and can be explained by a high proportion of aqueous fluid derived from a mixed altered crust–sediment source but with the crustal source dominant.

Nelson seamount, however, lies below the crust–mantle mixing line and can only be modelled by invoking a concave mixing line. This requires that the Sr/Nd ratio of the subduction component is low. Moreover, this geometry of the diagram dictates that the line must intersect the sediment–crust mixing line close to the sediment composition. The exact trend will be a function of a number of variables, including the degree of depletion of the mantle wedge and the degree of depletion of the sediment and crust (resulting from an earlier history of loss of fluids with high Sr/Nd ratios) by the time the subducted plates heats up to the temperatures needed. As REE have a low solubility in aqueous fluids [45], this component is likely to have been a silicate melt or high-temperature siliceous fluid.

In the model presented, Nelson seamount is bracketed by two curves. Starting with an average wedge composition M2, the seamount composition can be explained by addition of several percent of a subducted sediment component containing high concentrations of Sr and Nd but low Sr/Nd ratios. Note that these requirements are robust even though neither the degree of depletion of mantle wedge nor the composition of partial melts of subducted sediment can be quantified.

This bimodality of subduction components in arc lavas (crust-derived aqueous fluid and sediment-derived melt) is well known (e.g. [43,44]), and may be sequential, with the melt added first and the aqueous fluid later. However, it is unusual here because the volcano with the large sediment melt component is so different from the other volcanoes of the arc, differing primarily in its slab-edge location. Interestingly, Fretzdorff et al. [46] used (^{230}Th/^{238}U) ratios to demonstrate this bimodality of subduction component in the subduction influenced back-arc segments, E4 being dominated by the sediment melt component and E8 the aqueous fluid component. Leat et al. [27] also identified dredge 158 from Segment E2 as having a sediment melt input.

The samples from segments E2 (dredge 158) and E8 can therefore be modelled by the same trend as Nelson by mixing of a sediment-derived subduction component to the mantle wedge, though the back-arc locations mean that the proportion of that component is much smaller. Thus, the melt component can be added elsewhere in the system, though it is only at Nelson where it is so dominant.

The importance of Nd in distinguishing between the different subduction components is emphasized by the plot of ^{143}Nd/^{144} Nd versus Th/Nd in Fig. 6. The South American–Antarctic Ridge gives a steep MORB trend representing the composition of mantle of varying degrees of enrichment. Lavas from the main volcanic arc form a shallow trend (trend A, Fig. 6). By contrast, Nelson seamount gives a steeper trend which requires a Th/Nd ratio of about 0.48. This is significantly greater than the ratio in the sediment, indicating that Th is more incompatible than Nd during the sediment dehydration or melting episode. Samples from Segment E4 and dredge DR.158 from Segment 2 also plot on this same trend, confirming that the sediment component is a regional feature and that it is of similar Th and Nd content in both north and south.

The question of whether the component is a high-temperature aqueous fluid or melt is difficult to resolve. The straight line mixing between mantle and sediment in Fig. 6 demonstrates that the shallow trend A cannot result from addition of Th- and Nd-bearing sediment melt to sub-arc mantle. This trend must result from a phase carrying Th but little Nd. This is likely to be an aqueous fluid, as experimental data show that Th has fluid/mantle mineral distribution coefficients of approximately 0.1 to 16: high enough to transport significant amounts of Th though not as high as those of Rb, Ba and Pb [45,47,48]. On the other hand, trend B represents transport of both Th and Nd and is therefore more likely to be a silicate melt.

It could be argued that the Nelson Seamount dacite is a product of assimilation of sediment during the rise of magma through the crust, or of fusion of a basalt–sediment mixture in the arc crust. However, there is very strong evidence that the South Sandwich arc is non-accreting, such that >95% of sediment entering

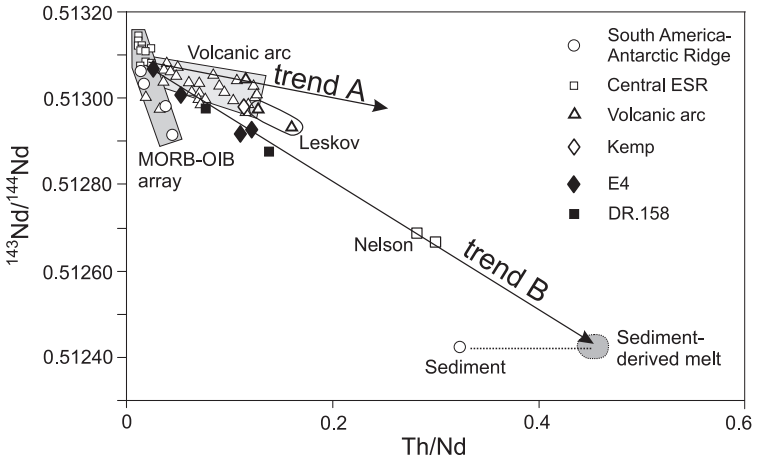

Fig. 6. Plot of $^{143}Nd/^{144}Nd$ versus Th/Nd for samples from the South Sandwich arc and back-arc, and the regional MORB-OIB array. Data sources as in Figs. 4 and 5. The diagram shows that Nd and Th are carried by different components. One dominates Th transport to the arc (trend A), while the other is responsible for Nelson samples and segments E4 and E2 (DR.158), and is probably a silicate melt the subducted sediments (trend B).

the trench during the last 15 million years has been subducted [17]. It is therefore unlikely that sufficient volumes of accreted sediment exist in the arc crust. Moreover, basalt–sediment mixing cannot model the Sr–Nd isotope characteristics of the Nelson dacites (Fig. 5).

7. Interpretation: processes at the subducting plate edges

We suggest that several processes are important at the slab edges of the South Sandwich system (Fig. 7).

7.1. Mantle flow around the slab ends

The mantle sampled by basalts in segments E2, E9, E10, and in sample DR.56.4 from E1, differs from the mantle sampled in the central segments by having higher ratios of Nb, Ba and Th relative to Yb, and generally lower $^{143}Nd/^{144}Nd$ and higher $^{87}Sr/^{86}Sr$ ratios, i.e. by being E-type, rather than N-type MORB. As others have already shown, the basalts from the edge and centre of the back-arc basin have isotopic affinities with the mantle domain influenced by the Bouvet plume [26,27,40,49,50], not from South Atlantic domains influenced by the Tristan, Discovery or Shona plumes [41,51] nor from mantle flowing east from the Pacific as proposed by Alvarez [52]. Data thus suggest that mantle is flowing into the East Scotia Sea from north and south [9,25] in response to roll-back of the subducting slab towards the east and that it is the same mantle domain that is presently tapped by the South American–Antarctic Ridge. The data also imply that the mantle is initially enriched (an E-MORB source) and that it becomes depleted (N-MORB source) as it becomes more distal from the basin edges.

The data also provide evidence that the mantle flow paths are different in the north and south edges. In the north, enriched mantle is tapped by the whole of Segment E2, and it appears to be entering the back-arc beneath this segment [27] (Fig. 7a). However, in the overwhelmingly depleted segment E1, enriched mantle is represented by just one sample. This segment is apparently not supplied by in-flowing, enriched mantle. This appears to be a result of its unusual position above the down-warped part of the non-subducting South American plate to the north of the tear. The mantle beneath Segment E1 cannot therefore be directly replenished by mantle flowing through the gap produced by the tearing plate (Fig. 7a). This constrains Segment E1 to be underlain by mantle that has been processed by previous melt extraction beneath more southerly segments or beneath the arc. We suggest that this accounts for its depleted nature. In contrast, at the south end of the system, the data provide evidence that both segments E9 and E10 are

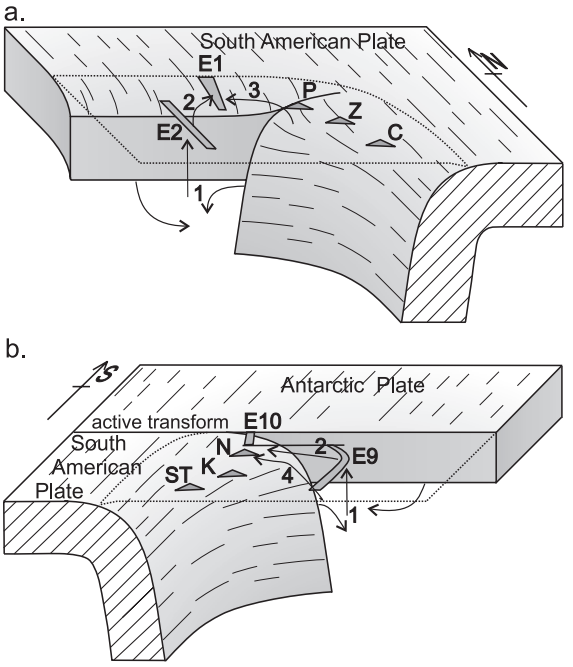

Fig. 7. Schematic cartoon of the northern and southern ends of the South Sandwich subduction system, showing key elements of interpreted mantle flow. The South American and Antarctic plates are shown to full thickness. The tops of the Scotia and Sandwich plates are depicted by dashed lines. (a) The northern part of the system, showing the down-warp in the South American Plate caused by tearing at the north end of the slab. Segment E1 overlies this down-warp. Mantle flows from east to west around the end of the slab (1), feeding Segment E2 with enriched mantle. Mantle arrives under segment E1 after having been depleted by melting beneath either segment E2 (2) or the arc (3). P, Protector Shoal; Z, Zavadovski; C, Candlemas. (b) The southern part of the system showing the transform between the South American and Antarctic plates. Mantle has unrestricted access to the southern back-arc from around the edge of the slab and from beneath the Antarctic Plate (1). Mantle arrives under Segment E10 having been depleted under Segment E9 (2), or directly around the slab edge (4). Hot mantle flowing along the slab edge may contribute to melting of sediments below Nelson Seamount. N, Nelson Seamount; K, Kemp Seamount; ST, Southern Thule.

enriched by mantle flowing around the slab edge. The southern slab edge follows a pre-existing transform fault, and there is no down-warping of the non-subducting slab and thus no barrier to flow. In-flowing enriched mantle can therefore supply both segments (Fig. 7b).

The same contrast might be applied to the arc itself. In the north, the northernmost arc volcano (Protector) has no unusual characteristics. Essentially, mantle has to flow eastwards before it reaches the zone of melting. In the south, the seamounts Nelson and Kemp can be fed by mantle flowing into the wedge from the side. This may help explain why Nelson plots on an extension of the arc array to higher Nb/Yb ratios and why Kemp has lower Nb/Yb ratios than Nelson.

7.2. Convergence of the arc with the back-arc spreading centre

Although the mantle flowing into the arc-basin system may have no subduction component, it is apparent that it rapidly obtains this component once it flows above the subducting plate. Thus, all samples from Segment E2 have a small subduction component while some (the low-Na group) have a larger component [27]. The new data presented here also demonstrate that, as well as becoming depleted, the mantle gains a further subduction component as it flows further towards segment E1. The data also demonstrate that, to a first approximation, Segment E9 is very similar to E2 in its elemental and isotopic characteristics, and this would be expected from its comparable setting above the plate edge. Basalts from Segment 10 are only slightly more depleted than E9, but have a larger subduction component. This is in keeping with the fact that E10 is nearer to the trench than E9 and is therefore likely to have a larger subduction flux. It is less fertile than its equivalent in the north (E1) because there is no barrier to influx of fertile mantle. However, E10 is similar to E1 in having a larger subduction component than the segment to its rear (E9 cf. E2) as measured by Ba and Th relative to Nb, and by Sr relative to Nd isotopes.

The ends of the back-arc spreading centre are nearer to the subducting slab and the arc than its central portions, and therefore are expected to have a stronger subduction zone signature and to be magmatically more robust [53]. This is partly the case in the East Scotia Sea. For example, the central segments (E5–E7) have no, or very small, subduction signals, and the strongest subduction inputs tend to be in segments near the slab ends. However, there are complexities, as segments E8 and E4 have large subduction signals [26]. Possibly, mantle feeding segments near the slab edges must flow over the

subducting slab, whereas mantle flowing into the centre of the basin has a trajectory which is more distal to the trench. Mantle recycled within the system may attain a greater subduction signal.

7.3. Anomalous heating and anomalous fluxes at the slab edges

Edges of subducting slabs are subject to anomalous thermal gradients. In the South Sandwich system, there is no evidence that the basaltic part of the slab edge has melted to produce adakites, as proposed for the Pacific plate edge subducting beneath Kamchatka [11]. Instead, we propose that subducting sediment melted at the southern edge of the slab in the South Sandwich system, and that this melt was a major component of the Nelson Seamount magmas. We propose that the sediment melting was caused by high temperatures along the edge of the slab.

In laboratory experiments [54], mantle flow around slab edges and its effect on surface temperatures of slabs has been modelled for the two cases of fixed slab position and slab roll-back. Subduction of slabs in fixed position was shown to lead to heating of slab ends relative to slab centres. Conversely, roll-back of slabs led to flow around slab edges and heating of slab centres faster than slab edges. If, as we propose, the melting of subducted sediments to produce the Nelson Seamount magma compositions was a result of higher-than-normal heating of the southern end of the slab beneath the South Sandwich arc, this is inconsistent with the laboratory experiments for the case of roll-back. We suspect that important factors in promoting melting of sediment or igneous rocks at the slab edge may be the increased surface area exposed to heating at the slab edge relative to its centre, and the high temperature of inflowing mantle relative to wedge mantle.

We are unsure why Kemp seamount acquired its distinctive, high Ba/Yb (relative to Nb/Yb) signature, implying a greater-than-normal input from aqueous fluids derived from the slab. Kemp Seamount is close to the south edge of the slab, and we speculate that the high Ba input to the mantle source may be related either to the high thermal gradient in the slab, or to a long trajectory of mantle flow. In the latter case, mantle flowing at an oblique angle to the trench would follow a pathway which would enable it to pick up more subduction component for a given amount of decompression.

7.4. Global comparisons

Comparisons with other subduction systems where slab edges are exposed reveal both similarities and differences. The two rock types most closely associated with slab edges are boninites and adakites, so we have evaluated these in more detail.

Boninites are common features of slab edges in southern Vanuatu and north Tonga. In the better-studied Tonga case, hot, plume mantle depleted under Samoa flows from the Pacific side of the slab into the back-arc leads to the eruption of high-Ca boninites [55,56]. Samples from segments E9, E10 or E2 are all tholeiitic basalts derived from non-depleted sources. The only possible boninite analogues from the back-arc edge segments in the East Scotia Sea are therefore samples from Segment E1. Common features of both these samples and boninites are subduction components added to depleted sources. However, in detail, none of the samples analysed here has boninite characteristics according to the various definitions. For example, although the unaltered sample DR.56.9 (the closest to a boninite) has a MgO value of 9.10 wt.% and SiO_2 value of 53.59 wt.%, it still plots just outside the boninite field [57], and its TiO_2 concentration of 0.59 wt.% exceeds the recommended upper bound of 0.5 wt.% [58]. The presence of boninites in North Tonga and tholeiites in north East Scotia may reflect differences in the mantle source: hot and depleted at the Samoan mantle plume in the former, cooler and depleted in the back-arc system in the latter. Possibly the best analogue for E1 is therefore with the depleted tholeiites recovered from the southern edge of the Mariana arc [59].

Note that the northernmost islands in the Tonga arc, and the southernmost in the Vanuatu arc [60] also have unusual geochemical characteristics attributed to addition of subduction components to ultra-depleted mantle sources. There is no direct analogue in the South Sandwich islands: neither Protector in the north nor Nelson and Kemp in the south require unusually depleted sources to explain their compositions.

Beneath Kamchatka, anomalously high heating of a slab edge has melted basaltic crust of the underlying

plate to produce adakites [11]. In the South Sandwich arc, both the northernmost volcano (Protector) and the southernmost (Nelson) are dacitic, but neither are adakitic. Although Nelson seamount has been interpreted here as requiring a sediment melt component, it has high Y contents (26–31 ppm) and low Sr/Y ratios (5–6) which places it in well inside the normal arc field of Defant and Drummond [61]. The melting of sediment beneath Nelson seamount rather than the igneous slab beneath Kamchatka is an important distinction between the South Sandwich and Kamchatka cases. The difference may be related to the slower roll-back of the Kamchatka slab allowing greater heating of the slab ends, or to the relative absence of sediment beneath Kamchatka so that crust rather than sediment encounters the high, shear-assisted, temperature of the slab-wedge interface. In both cases, however, the geometry of the slab edge appears to have been critical in producing the melting.

There may thus be closer similarities between Nelson seamount at the southern edge of the South Sandwich arc and Grenada at the southern end of the Lesser Antilles arc. Both have exceptional enrichment in elements such as Th, which may be attributed to sediment melting, although Grenada has high Na and is alkalic in composition whereas Nelson is not. Moreover, the proximity to the South American margin means that there is much greater flux of sediment into the southern Lesser Antilles arc; the sediment flux beneath Nelson is much smaller.

8. Conclusions

The ends of the South Sandwich arc and back-arc show distinctive magma chemistries that indicate that processes at the edges of the subducting slab have a strong influence on magma genesis. These processes are: roll-back of the slab, forcing mantle inflow to the mantle wedge around the edges of the slab; the physical convergence of the arc with the back-arc spreading centre at the two ends of the subduction zone, producing arc-like magmas within the back-arc; and anomalous heating of the edges of the slab, causing sediment melts to contribute to arc magmas.

Acknowledgements

This work is funded by the NERC Antarctic Funding Initiative (grant No. AFI2/36) and Joint Infrastructure Fund (grant No. NER/H/S/2000/00862). We thank Susanne Fretzdorff for providing microprobe data. We thank J. Gamble, P. Stoffers and S. Fretzdorff for useful comments.

Appendix A. Supplementary data

Supplementary data associated with this article can be found, in the online version, at doi:10.1016/j.epsl.2004.08.016.

References

[1] Y. Tatsumi, Migration of fluid phases and genesis of basalt magmas in subduction zones, J. Geophys. Res. 94 (1989) 4697–4707.
[2] J.H. Davies, D.J. Stevenson, Physical model of source region of subduction zone volcanics, J. Geophys. Res. 97 (1992) 2037–2070.
[3] J.A. Pearce, D.W. Peate, Tectonic implications of the composition of volcanic arc magmas, Annu. Rev. Earth Planet. Sci. 23 (1995) 251–285.
[4] Y. Tatsumi, S. Eggins, Subduction Zone Magmatism, Blackwell Science, Cambridge, MA, 1995, p. 211.
[5] R.M. Russo, P.G. Silver, Trench-parallel flow beneath the Nazca plate from seismic anisotropy, Science 263 (1994) 1105–1111.
[6] G.P. Smith, D.A. Wiens, K.M. Fisher, L.M. Dorman, S.C. Webb, J.A. Hildebrand, A complex pattern of mantle flow in the Lau backarc, Science 292 (2001) 713–716.
[7] M. Bevis, F.W. Taylor, B.E. Schutz, J. Recy, B.L. Isacks, S. Helu, R. Singh, E. Kendrick, J. Stowell, B. Taylor, S. Calmant, Geodetic observations of very rapid convergence and back-arc extension at the Tonga arc, Nature 374 (1995) 249–251.
[8] J. Dvorkin, A. Nur, G. Mavko, Z. Benavraham, Narrow subducting slabs and the origin of backarc basins, Tectonophysics 227 (1993) 63–79.
[9] R.A. Livermore, A. Cunningham, L. Vanneste, R. Larter, Subduction influence on magma supply at the East Scotia Ridge, Earth Planet. Sci. Lett. 150 (1997) 261–275.
[10] S. Turner, C. Hawkesworth, Using geochemistry to map mantle flow beneath the Lau Basin, Geology 26 (1998) 1019–1022.
[11] G.M. Yogodzinski, J.M. Lees, T.G. Churikova, F. Dorendorf, G. Woerner, O.N. Volynets, Geochemical evidence for the melting of subducting ocean lithosphere at plate edges, Nature 409 (2001) 500–504.
[12] A. Deschamps, S. Lallemand, Geodynamic setting of Izu-Bonin-Mariana boninites, in: R.D. Larter, P.T. Leat (Eds.), Intra-Oceanic Subduction Systems: Tectonic and Magmatic

Processes, Geol. Soc. London Spec. Publ. 219 (2003) 163–185.
[13] S.E. DeLong, F.N. Hodges, R.J. Arculus, Ultramafic and mafic inclusions, Kanaga Island, Alaska, and the occurrence of alkaline rocks in island arcs, J. Geol. 83 (1975) 721–736.
[14] M.F. Thirlwall, A.M. Graham, R.J. Arculus, R.S. Harmon, C.G. Macpherson, Resolution of the effects of crustal assimilation, sediment subduction, and fluid transport in island arc magmas: Pb–Sr–Nd–O isotope geochemistry of Grenada, Lesser Antilles, Geochim. Cosmochim. Acta 60 (1996) 4785–4810.
[15] P.F. Barker, L.A. Lawver, South American–Antarctic plate motion over the past 50 Ma, and the evolution of the South American–Antarctic Ridge, Geophys. J. R. Astron. Soc. 94 (1988) 377–386.
[16] R.A. Livermore, R.W. Woollett, Seafloor spreading in the Weddell Sea and southwest Atlantic since the Late Cretaceous, Earth Planet. Sci. Lett. 117 (1993) 475–495.
[17] L.E. Vanneste, R.D. Larter, Sediment subduction, subduction erosion and strain regime in the northern South Sandwich forearc, J. Geophys. Res. 107 (B7) (2002) 2149.
[18] C. Thomas, R.A. Livermore, F.F. Pollitz, Motion of the Scotia Sea plates, Geophys. J. Int. 155 (2003) 789–804.
[19] C.P. Brett, Seismicity of the South Sandwich Islands region, Geophys. J. R. Astron. Soc. 51 (1977) 453–464.
[20] D.W. Forsyth, Fault plane solutions and tectonics of the South Atlantic and Scotia Sea, J. Geophys. Res. 80 (1975) 1429–1443.
[21] P.F. Barker, Tectonic framework of the East Scotia Sea, in: B. Taylor (Ed.), Barckarc Basins: Tectonics and Magmatism, Plenum Press, New York, 1995, pp. 281–314.
[22] R.D. Larter, L.E. Vanneste, P. Morris, D.K. Smyth, Tectonic evolution and structure of the South Sandwich arc, in: R.D. Larter, P.T. Leat (Eds.), Intra-Oceanic Subduction Systems: Tectonic and Magmatic Processes, Geol. Soc. London Spec. Publ. 219 (2003) 255–284.
[23] J.A. Pearce, P.E. Baker, P.K. Harvey, I.W. Luff, Geochemical evidence for subduction fluxes, mantle melting and fractional crystallization beneath the South Sandwich arc, J. Petrol. 36 (1995) 1073–1109.
[24] P.T. Leat, J.L. Smellie, I.L. Millar, R.D. Larter, Magmatism in the South Sandwich arc, in: R.D. Larter, P.T. Leat (Eds.), Intra-Oceanic Subduction Systems: Tectonic and Magmatic Processes, Geol. Soc. London Spec. Publ. 219 (2003) 285–313.
[25] R. Livermore, Back-arc spreading and mantle flow in the east Scotia Sea, in: R.D. Larter, P.T. Leat (Eds.), Intra-Oceanic Subduction Systems: Tectonic and Magmatic Processes, Geol. Soc. London Spec. Publ. 219 (2003) 315–331.
[26] S. Fretzdorff, R.A. Livermore, C.W. Devey, P.T. Leat, P. Stoffers, Petrogenesis of the back-arc East Scotia Ridge, South Atlantic Ocean, J. Petrol. 43 (2002) 1435–1467.
[27] P.T. Leat, R.A. Livermore, I.L. Millar, J.A. Pearce, Magma supply in back-arc spreading centre segment E2, East Scotia Ridge, J. Petrol. 41 (2000) 845–866.
[28] N.J. Bruguier, R.A. Livermore, Enhanced magma supply at the southern East Scotia Ridge: evidence for mantle flow around the subducting slab? Earth Planet. Sci. Lett. 191 (2001) 129–144.
[29] C. Müller, Upper mantle seismic anisotropy beneath Antarctica and the Scotia Sea region, Geophys. J. Int. 147 (2001) 105–122.
[30] P.F. Barker, I.A. Hill, S.D. Weaver, R.J. Pankhurst, The origin of the eastern South Scotia ridge as an intraoceanic island arc, in: C. Craddock (Ed.), Antarctic Geoscience, University of Wisconsin Press, Madison, 1982, pp. 203–211.
[31] P.F. Barker, P.L. Barber, E.C. King, An early Miocene ridge crest–trench collision on the South Scotia Ridge near 36°W, Tectonophysics 102 (1984) 315–332.
[32] R.J. Pankhurst, C.R. Rapela, Production of Jurassic rhyolites by anatexis of the lower crust of Patagonia, Earth Planet. Sci. Lett. 134 (1995) 23–36.
[33] C.J. Hawkesworth, R.K. O'Nions, R.J. Pankhurst, P.J. Hamilton, N.M. Evensen, A geochemical study of island arc and back-arc tholeiites from the Scotia Sea, Earth Planet. Sci. Lett. 36 (1977) 253–262.
[34] A.D. Saunders, J. Tarney, The geochemistry of basalts from a back-arc spreading centre in the east Scotia Sea, Geochim. Cosmochim. Acta 43 (1979) 555–572.
[35] D.W. Meunow, N.W.K. Liu, M. Garcia, A.D. Saunders, Volatiles in submarine volcanic rocks from the spreading centre axis of the east Scotia Sea back-arc basin, Earth Planet. Sci. Lett. 47 (1980) 272–278.
[36] R.S. Cohen, R.K. O'Nions, Identification of recycled continental material in the mantle from Sr, Nd and Pb isotope investigations, Earth Planet. Sci. Lett. 61 (1982) 73–84.
[37] A.D. Saunders, J. Tarney, S.D. Weaver, P.F. Barker, Scotia Sea floor: geochemistry of basalts from the Drake Passage and South Sandwich spreading centres, in: C. Craddock (Ed.), Antarctic Geoscience, University of Wisconsin Press, Madison, 1982, pp. 213–222.
[38] D.P. Mattey, R.H. Carr, I.P. Wright, C.T. Pillinger, Carbon isotopes in submarine basalts, Earth Planet. Sci. Lett. 70 (1984) 196–206.
[39] I.W. Hamilton, Geophysical investigations of subduction-related processes in the Scotia Sea, unpub. PhD thesis, University of Birmingham, 1989.
[40] J.A. Pearce, P.T. Leat, P.F. Barker, I.L. Millar, Geochemical tracing of Pacific-to-Atlantic upper mantle flow through the Drake Passage, Nature 410 (2001) 457–461.
[41] P.J. le Roux, A.P. le Roex, J.-G. Schilling, N. Shimizu, W.W. Perkins, N.J.G. Pearce, Mantle heterogeneity beneath the southern Mid-Atlantic ridge: trace element evidence for contamination of ambient asthenospheric mantle, Earth Planet. Sci. Lett. 203 (2002) 479–498.
[42] S.-S. Sun, W.F. McDonough, Chemical and isotopic systematics of oceanic basalts: implications for mantle composition and processes, in: A.D. Saunders, M.J. Norry (Eds.), Magmatism in the Ocean Basins, Geol. Soc. London Spec. Publ. 42 (1989) 313–345.
[43] T. Elliott, T. Plank, A. Zindler, W. White, B. Bourdon, Element transport from slab to volcanic front at the Mariana arc, J. Geophys. Res. 102 (1997) 14991–15019.

[44] C.J. Hawkesworth, S.P. Turner, F. McDermott, D.W. Peate, P. van Calsteren, U–Th isotopes in arc magmas: implications for element transfer from the subducted crust, Science 276 (1997) 551–555.
[45] H. Keppler, Constraints from partitioning experiments on the composition of subduction zone fluids, Nature 380 (1996) 237–240.
[46] S. Fretzdorff, K.M. Haase, P.T. Leat, R.A. Livermore, C.-D. Garbe-Schönberg, J. Fietzke, P. Stoffers, ^{230}Th–^{238}U disequilibrium in East Scotia back-arc basalts: implications for slab contributions, Geology 31 (2003) 693–696.
[47] J.M. Brenan, H.F. Shaw, F.J. Ryerson, D.L. Phinney, Mineral–aqueous fluid partitioning of trace elements at 900 °C and 2.0 GPa: constraints on the trace element chemistry of mantle and deep crustal fluids, Geochim. Cosmochim. Acta 59 (1995) 3331–3350.
[48] M.C. Johnson, T. Plank, Dehydration and melting experiments constrain the fate of subducted sediments, Geochem. Geophys. Geosyst. 1 (1999) (1999GC000014).
[49] A.P. le Roex, H.J.B. Dick, A.M. Reid, F.A. Frey, A.J. Erlank, S.R. Hart, Petrology and geochemistry of basalts from the American–Antarctic Ridge, Southern Ocean: implications for the westward influence of the Bouvet mantle plume, Contrib. Mineral. Petrol. 90 (1985) 367–380.
[50] D. Harrison, P.T. Leat, P. Burnard, G. Turner, S. Fretzdorff, I.L. Millar, Resolving mantle components in oceanic lavas from segment E2 of the East Scotia back-arc ridge, South Sandwich Islands, in: R.D. Larter, P.T. Leat (Eds.), Intra-Oceanic Subduction Systems: Tectonic and Magmatic Processes, Geol. Soc. London Spec. Publ. 219 (2003) 333–344.
[51] J. Douglass, J.-G. Schilling, D. Fontignie, Plume–ridge interactions of the Discovery and Shona mantle plumes with the southern Mid-Atlantic Ridge (40°–55°S), J. Geophys. Res. 104 (1999) 2941–2962.
[52] W. Alvarez, Geological evidence for the geographical pattern of mantle return flow and the driving mechanism of plate tectonics, J. Geophys. Res. 87 (1982) 6697–6700.
[53] B. Taylor, F. Martinez, Back-arc basin systematics, Earth Planet. Sci. Lett. 210 (2003) 481–497.
[54] C. Kincaid, R.W. Griffiths, Laboratory models of the thermal evolution of the mantle during rollback subduction, Nature 425 (2003) 58–62.
[55] T.J. Falloon, A.J. Crawford, The petrogenesis of high-Ca boninite lavas dredged from the north Tonga Ridge, Earth Planet. Sci. Lett. 102 (1991) 375–394.
[56] L.V. Danyushevsky, S.V. Sobolev, T.J. Falloon, North Tongan high-Ca boninite petrogenesis: the role of Samoan plume and subduction zone-transform transition, J. Geodyn. 20 (1995) 219–241.
[57] R.J. Arculus, J.A. Pearce, B.J. Murton, S.R. van der Laan, Igneous stratigraphy and major-element geochemistry of Holes 786A and 786B, ODP Sci. Rep. 125 (1992) 143–169.
[58] A.J. Crawford, T.J. Fallon, D.H. Green, Classification, petrogenesis and tectonic setting of boninites, in: A.J. Crawford (Ed.), Boninites, Unwin Hyman, London, 1989, pp. 1–49.
[59] A.J. Crawford, L. Beccaluva, G. Serri, J. Dostal, Petrology, geochemistry and tectonic implications of volcanics dredged from the intersection of the Yap and Mariana trenches, Earth Planet. Sci. Lett. 80 (1986) 265–280.
[60] M. Monzier, L.V. Danyushevsky, A.J. Crawford, H. Bellon, J. Cotton, High-Mg andesites from the southern termination of the New Hebrides island arc (SW Pacific), J. Volcanol. Geotherm. Res. 57 (1993) 193–217.
[61] M.J. Defant, M.S. Drummond, Derivation of some modern arc magmas by melting of young subducted lithosphere, Nature 347 (1990) 662–665.
[62] D.T. Sandwell, W.H.F. Smith, Martine gravity anomaly from Geosat and ERS 1 satellite altimetry, J. Geophys. Res. 102 (1997) 10039–10954.